International Journal of Cardiac Imaging **13:** 347–355, 1997.

Automated detection of the left ventricular region in magnetic resonance images by Fuzzy *C*-Means model

Abd-El-Ouahab Boudraa
Laboratoire de Biophysique, Faculté de Médecine René Laënnec, rue Guillaume Paradin 69372 Lyon, France

Accepted 2 October 1996

Key words: magnetic resonance images, fuzzy sets, optimization, fuzzy clustering, segmentation

Abstract

A new method for automated detection of the Left Ventricular (LV) region in Magnetic Resonance Imaging is presented. This method is based on the Fuzzy *c*-Means (FCM) clustering algorithm. The FCM is applied to each static frame of the cardiac cycle to detect the LV region. Delineation of this region is essential in the quantitative analysis of the cardiac function. The effectiveness of the method is demonstrated by application to sequences of cardiac images.

Introduction

The aim of pattern recognition is to partition data into a certain number of clusters or 'natural groups'. The elements inside each cluster are as similar as possible to each other and as different as possible from those of the other sets. One means of organizing unlabeled objects in a multi-dimensional space into meaningful subsets or clusters is to use clustering algorithms. These techniques optimize an objective function based on a similarity measure between the elements of the space and each of the cluster centers. These techniques have found application in medical imaging, life sciences, information and decision sciences, and engineering. In medical imaging, these algorithms have gained popularity for the segmentation of Magnetic Resonance (MR) data to provide quantitative information for clinical analysis. The application of MR imaging to the cardiovascular system has offered new non-invasive means for the assessment of the cardiac function [1]. The objective is to obtain a reasonable number of well-segmented regions that have good correlation with the anatomy. Indeed, the adequate delineation of the left ventricular region, in gated cardiac MR imaging, is important to estimate parameters of cardiac function such as ventricular volume and ejection fraction. These global parameters provide important prognostic information in heart disease. This task can be performed by outlining the Left Ventricle (LV) interactively on a computer screen by the operator using a mouse or track ball as an input device. The disadvantage of this method is that it can result in large intra- and inter-observers variability and this leads to uncorrect detection of the LV edges. Thus, an automated approach for reliable and robust segmentation results is more suitable. Several automatic and semiautomatic methods have been proposed [2–10]. To extract data from cardiac images, these methods use thresholding and contour following procedures [2], thresholding and zero-crossings of the second derivative of the image procedures [3], active contour models [4, 5], a parametric deformable model based on elliptic Fourier decomposition [6], relaxation labeling [7], the Dempster-Shafer theory [8], graph searching [9] and dynamic programming [10].

In the standard approach, most segmentation algorithms [11–13] assume that each pixel (or voxel) belongs to a single cluster or tissue type. However, the complexity of tissue boundaries causes many voxels to contain a mixture of surrounding tissues (partial volume effects). Thus, image ambiguity within pixels is due to the possible multi-valued levels of brightness in the image. This indeterminacy is due to inherent vagueness rather than randomness. Since image regions are not always crisply defined, it becomes more convenient and appropriate to regard them as fuzzy subsets of the image [14, 15]. The fuzzy subsets are characterized by

the possibility (degree) of belonging of each pixel to them. One popular method for assigning multi-subset membership values to pixels, for either segmentation or other types of processing, is the Fuzzy *c*-Means (FCM) algorithm [16].

The automatic detection of the LV contours by hard clustering (e.g. ISODATA clustering methods) is difficult due to the fuzziness of pixel information. Thus, a method based on the FCM algorithm for outlining correctly the LV is believed to be suitable for overcoming this problem. This approach has been successfully used to solve detection problems in other medical applications [17–19].

This paper is organized as follows: Section 2 presents the mathematical formulation of the problem and the associated notations and the recognition of the LV region procedure (Method). Preliminary computational results and discussions are presented in Sections 3 and 4, respectively. Finally, we give some conclusions in Section 5.

Method

The proposed method consists of segmenting the cardiac image into clusters and in identifying the LV region using a pattern recognition procedure.

The FCM partitioning model

Given a finite set of data points, $X = x_1,\ldots,x_n$, the FCM algorithm minimizes the weighted within groups sum of squared errors objective function [16].

$$Jm(U,V;X) = \sum_{k=1}^{n} \sum_{i=1}^{c} (\mu_{ik})^m \cdot (d_{ik})^2$$

$$V = (v_1, v_2, ..., v_c)$$

subject to

$$\mu_{ik} \in [0,1]$$

$$\sum_{i=1}^{c} \mu_{ik} = 1 \;\; 1 \leq k \leq n$$

$$\sum_{k=1}^{n} \mu_{ik} \in]0,n[\;\; 1 \leq i \leq c.$$

where n is the number of data to be clustered, c the number of clusters and m a scalar, $m > 1$, measuring the degree of fuzzification. The larger the value of m, the less the effect of the data points producing uniformly low membership values on the determining of the clusters [20]. Consequently, these points tend to be ignored in determining the centers and membership functions. $x_k \in \mathbf{R}^p$ is a feature vector and $\mathbf{R}^p$ is the feature space. The real $n \times c$ matrix $U = \mu_{ik}$ is a fuzzy c-partition of X and each of its elements μ_{ik} is the membership degree of feature vector k to cluster i. $V = (v_1,v_2,...,v_c) \subseteq \mathbf{R}^{c \times p}$ with $v_i \in \mathbf{R}^p$ is the cluster center or prototype of the ith cluster. $d_{ik} = \| x_k - v_i \|_A$ is a measure of similarity between v_i and x_k with $\|.\|$ being any inner product induced norm on $\mathbf{R}^p$ and A any positive $(p \times p)$ matrix. Bezdek [16] proposed the FCM algorithm to solve the proposed minimization problem. The following is the statement of the algorithm. Let *lo* be a logical value, $\in$ a threshold value and c the number of clusters.

Step 1: $lo \leftarrow$ False
Choose any inner product induced norm metric $\|.\|_A$.

Step 2: Choose c clusters such that:
$\sum_{i=1}^{c} \mu_{ik} = 1.$

Step 3: Calculate the c clusters center
$$vi = \frac{\sum_{k=1}^{n} (\mu_{ik})^m . x^k}{\sum_{k=1}^{n} (\mu_{ik})^m}$$

Step 4: Compute new membership values:
$$\mu_{ik} = \frac{1}{\sum_{j=1}^{c} (\frac{d_{ik}}{d_{jk}})^{\frac{2}{(m-1)}}}$$
if $(lo = \text{False})\{$
$\tilde{v}_i \leftarrow vi$
$lo \leftarrow$ True
goto **Step 3** $\}$

Step 5: Compute the defect measure
$E = \sum_{i=1}^{c} \| \tilde{v}_i - v_i \|$
if $(E_t > \in)$
$\tilde{v}_i \leftarrow v_i$
goto > **Step 3**

Step 6: Defuzzification Process:
$\chi_k \in i \Leftrightarrow = arg(\frac{max}{1 \leq j \leq c}(\mu_{jk}))$

The above optimization procedure (**Step 1** to **Step 5**) is made by using the Lagrangian multiplier and can be found in Bezdek [16]. The **FCM** algorithm is globally convergent to either a local minimum or a saddle point of J_m [21].

Recognition Process (RP)

Since the gray level information alone is insufficient for development of an automated detection method, the spatial information is added to the processing. The spatial and gray level information act synergistically. Measurement such as area, centroid and moment of inertia can be used to augment the limited gray level information captured in low-level segmentation. In our study, the centroid feature which contains positional information and is easy to compute, is used to identify the LV region. Note that the labeling order generated by the FCM is unpredicable. For example, for two different segmentations, a given region of the image might come out as the *i*th cluster in the first segmentation and as the *j*th ($j \neq i$) cluster in the second.

Because the MR cardiac images are often within the same orientation, the spatial position of various structures can be exploited. Thus, the relative position of the two ventricles can be used in identifying the LV region. Indeed, an important part of the LV cavity is located within the right half part of the image and the Right Ventricle (RV) in the left one. Furthermore, note that the highest gray levels of the image are found in the ventricular region. The maximum of the image gray levels, G_{max}, corresponds to a pixel belonging to the LV or RV region. Thus, the centroid feature and the maximum of gray levels are used to classify the LV region using the following pseudo-code.

RP1: Compute the centroid of each cluster $(x_c(l), y_c(l))$ $l \in \{2, ..., c\}$

RP2: $G_{\max} \leftarrow \frac{max(Sora_1(i,j))}{1 \leq i,j \leq 256}$

RP3: $\forall (i,j)$ If$(Sora_1(i,j) = G_{\max})$ Then
$l_1 \leftarrow Sora_2(i,j)$
goto RP4
End If

RP4: $\forall (i,j) \in \aleph_{l_1} Sora_1(i,j) \leftarrow 0$

RP5: $G_{\max} \leftarrow \frac{\max(\text{Sora}_1(\text{i,j}))}{1 \leq \text{i,j} \leq 256}$

RP6: $\forall (i,j) \notin \aleph_{l_1}$ If$(Sora_1(i,j) = G_{\max})$ Then
$l_2 \leftarrow Sora_2(i,j)$
goto RP7
End If

RP7: If$(x_c(l_1) > x_c(l_2))$
$l_{LV} \leftarrow l_1$
$l_{RV} \leftarrow l_2$
Else
$l_{LV} \leftarrow l_2$
$l_{RV} \leftarrow l_1$
End If

Sora$_1$() is the initial image. *Sora*2() is the segmented image and each of its elements corresponds to a cluster label. $\aleph_{l_1}$ is the set of points of the l_1^{th} cluster. l_{LV} and l_{RV} are the labels affected by the FCM to the LV and RV clusters respectively.

Results

Automatic segmentation of medical images has the potential to facilitate an imaging based diagnosis. Gated cardiac MR imaging technique is used to provide information concerning global and/or regional ventricular function. It provides an excellent contrast between the flowing blood and myocardium and offers a potential tool for determining both RV and LV volumes. The proposed method is tested on Short-Axis (SA) cardiac MR images of four patients. These images are generated using a superconducting magnet operating at 1.5 Tesla (Philips Gyroscan). LV function is evaluated using measurements obtained from Cine-MR imaging. This technique employed a flip angle of 30° and gradient refocused echoes with an echo time of 123 ms. ECG-gated multi-slice and multi-phase technique was used. The field of view and the slice thickness are of 350 mm and 10 mm, respectively. SA images are obtained at 10 different positions (slices) and 11 times intervals (phases) during the cardiac cycle. Thus, the heart is divided into 10 SA slices from the base to the apex. The results of applying the proposed method are presented in Figures 1–6. Figure 1A shows an example of SA cardiac image. Figure 1B displays the smoothing result of Figure 1A with a median filter (3×3). Notice that the filtering has attenuated the flow variations. Figure 2 shows 9 filtered cardiac images among 11 of the middle plane of the cardiac cavity corresponding to 9 phases. In each image, a C-shaped RV

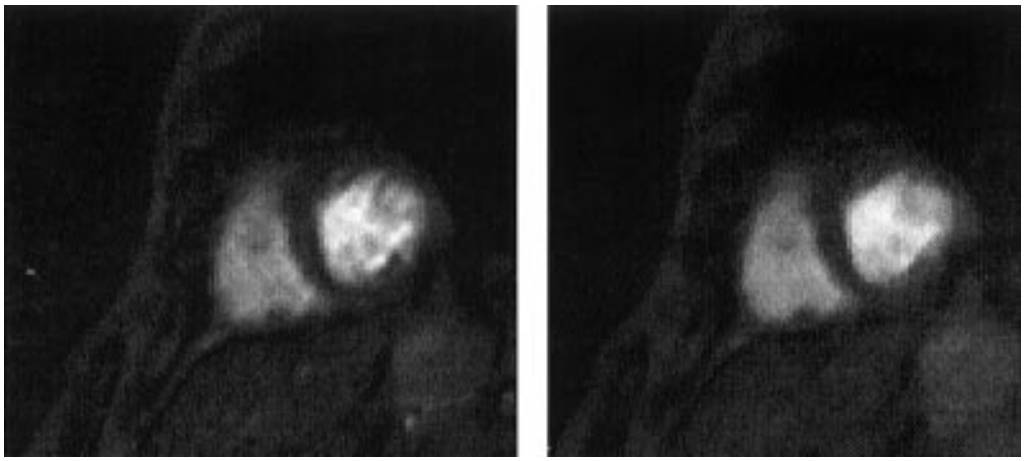

A B

Figure 1. MR image of the middle of the heart of patient 1 at end-diastole (a). Smoothing of (*A*) with a median filter (*B*).

drapes around an oval LV. Roughly speaking, for SA view and in the field of view chosen, one can see the following homogeneous regions: the LV, the RV, the spleen, the lung, the liver and the background image. Thus, one may choose $c = 6$ to divide the cardiac slice into its major constituents. In this study, the Euclidean inner product norm is used to compute the distance between vectors. A is the unit matrix. The fuzzy clustering is performed with threshold value $\in$ set to 10^{-3} [18]. For each phase of the cardiac cycle, the FCM is applied to the 10 slices, starting from the apex to the base of the heart. Thus, for each patient, 110 cardiac images are segmented. The CPU times of the FCM to generate a segmented image depends on the initializations of the membership degrees (Step 2). The FCM affects to each cluster (LV, RV, ...) a label which is unpredictable. To find the label assigned by the FCM to the LV or the RV cluster, the G_{max} value is searched. Since the blood pools of the LV and RV appear as the brightest regions, this information is used to determine G_{max} value which belongs to either the LV or the RV cluster. To ensure that the pixel of G_{max} value lies in the ventricular region, the highest pixel value of each slice of the cardiac cycle is searched and the median value of the obtained data points sequence is taken. The median is a robust parameter and is insensitive to unwanted spike noise value in the monotically increasing sequence. To guarantee that the label found by G_{max} value corresponds to the LV cluster, the relative position of the two ventricles is used. The centroid of each ventricle is calculated in all slices. It cannot be displayed by more than some threshold distance. By examining various image sequences, we have found that this displacement is never larger than two or three pixels and in all cases $x_c(LV) > x_c(RV)$. Table 1 shows the $x()$ values calculated in a sequence of 11 images (patient 1).

Table 1. X-coordinate of the LV and RV centroids in a sequence of filtered cardiac images

Slice number	X(LV)	X(RV)
1	57.122	30.897
2	57.024	32.042
3	55.890	32.278
4	54.425	32.535
5	53.891	32.799
6	53.268	33.734
7	55.169	33.908
8	55.779	33.894
9	56.024	34.112
10	56.785	34.789
11	57.122	35.267

The fuzzy clustering is performed in a reduced space. The ventricular area is narrowed to a limited space of the initial image. Thus, from each 256 $\times$ 256 filtered image, a 128 $\times$ 128 window delimiting the ventricular region is selected. This preprocessing step eliminates unnecessary information and reduces the computing time to about 70%. The comparison of the initial images (Figure 2) and the segmented ones (Figure 3) shows that the LV endocardial edges are well delineated. This is also well illustrated in Figure 4 where the edges of the trabeculated LV are, for example, difficult to delineate by a manual tracing. For the remaining three patients image sequences, the

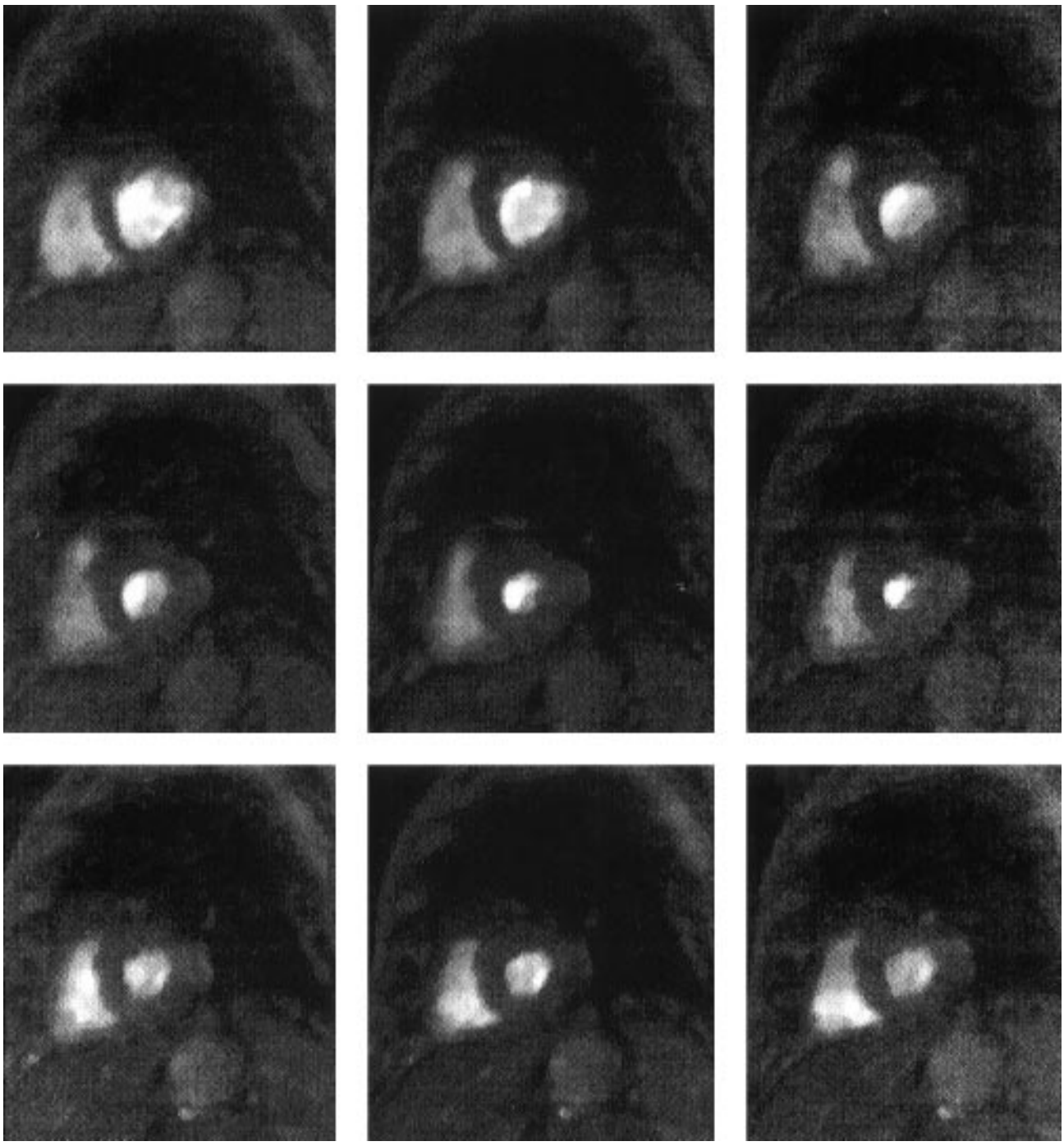

Figure 2. A sequence of nine filtered MR images taken throughout the cardiac cycle.

same processing procedures (filtering and clustering) are applied as in patient 1. For each phase of the cardiac cycle, the different cross-sectional areas of the LV are calculated. Volumes are estimated for each phase by adding the areas multiplied by slice thickness and the LV function curve calculated (Figure 5). This curve shows the change in ventricular blood volume during the cardiac cycle. The maximum and the minimum

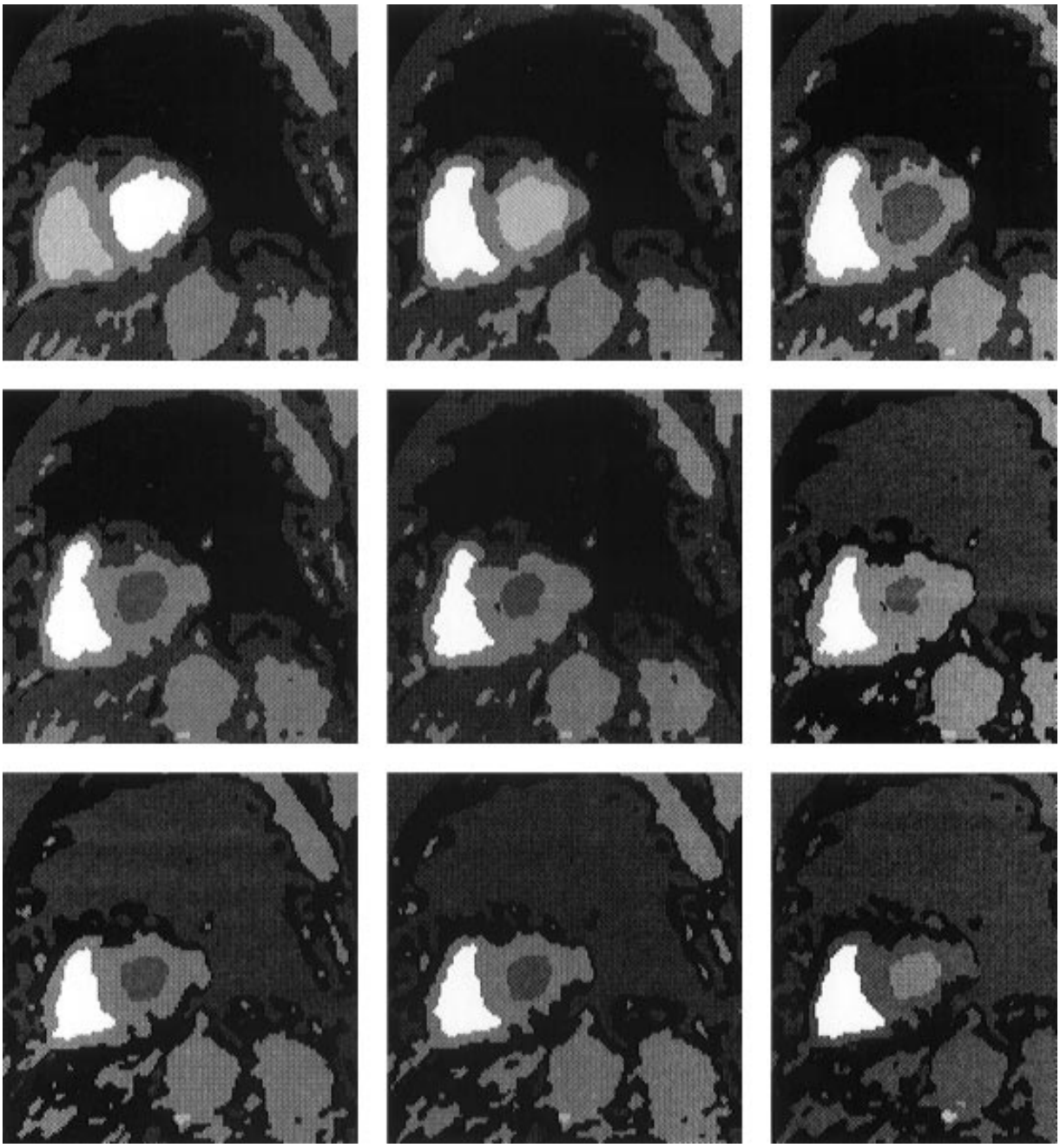

Figure 3. Fuzzy clustering results of a sequence of nine filtered MR images.

of this curve correspond to the end-diastole and the end-systole phases, respectively. The cardiac EF is determined by substracting the end-diastolic volume from the end-systolic volume and dividing by the end-diastolic volume.

The performance of the edges detection algorithm is evaluated both qualitatively and quantitatively. In order to assess qualitatively the performance of the contour extraction algorithm, the results are given to a trained radiologist for visual evaluation. Each segmented image is scored and an average score is calculated

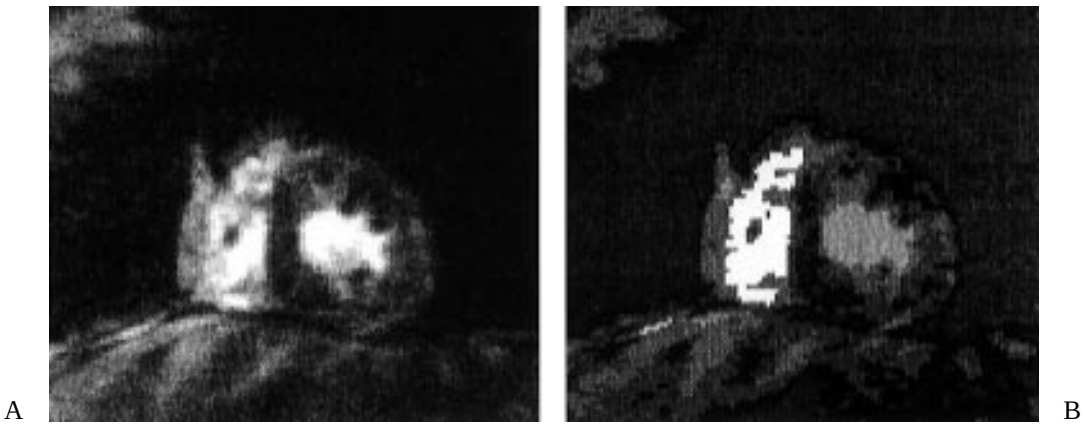

Figure 4. MR image of the middle of the heart of patient 2 at end-diastole. Smoothing of (A) with a median filter (B).

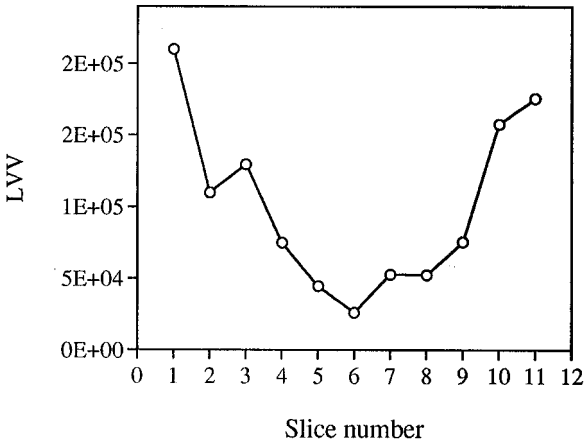

Figure 5. Left ventricular function curve (patient 1).

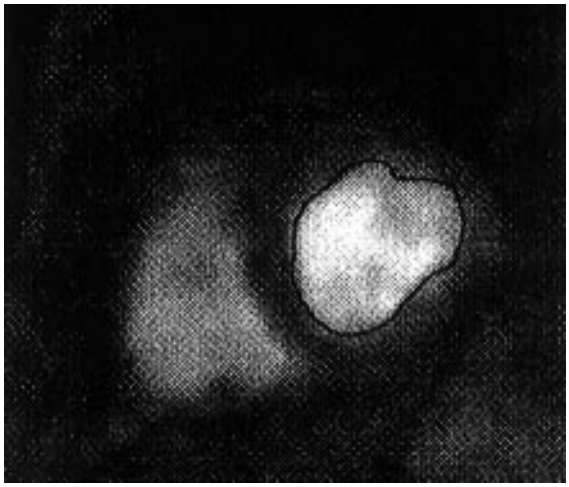

Figure 6. Expert's hand drawn contours of end-diastolic MR image of the middle of the heart (patient 1).

Table 2. Ejection fractions obtained by the FCM based method and from the expert's hand drawn contours

Patient	Expert (%)	FCM (%)
1	65	70
2	45	40
3	49	55
4	20	16

for each patient. The qualitative evaluation led to 85% visually acceptable contours in patients 1 and 3 and 65% and 75% in patients 2 and 4 respectively giving an average visual accuracy of 77%. In order to evaluate quantitatively the accuracy of the proposed method, automatically obtained EFs are compared with those determined by manual tracing. Studies have demonstrated the reliability of manual tracing in determination of the left ventricular boundaries in MR images [22–24]. Ventricular boundaries of Figure 1B manually traced by an experienced radiologist is shown in Figure 6. The manual tracing is performed without having previously seen the automatically obtained edges. Then, the areas enclosed by the manually traced endocardium are computed, and the EFs estimated (Table 2). As can be observed, the EFs given by the FCM are in agreement with those giving by the manual method. The average difference between these EFs is of 5%.

Discussion

The Cine-MR imaging depicts flowing blood as a bright signal. The blood pool shows high signal

imaging intensity in all phases of the cardiac cycle. Although blood in the cardiac chambers appears as bright regions, it does not have homogeneous intensities. Indeed, the velocity of intraventricular blood varies not only during the cardiac cycle but also with its location within the ventricles. Since the brightness of blood varies with its flow velocity, variations in intensity are observed in the ventricular blood. Thus, a smoothing is used to reduce intensity variations in the blood pools. As can be observed, the image after smoothing still shows the blood pools as the brightest regions (Figure 1B). If the filter is applied more than twice, the LV and the RV may merge into one. Note that if a clustering is performed on a non-filtered image the FCM breaks the LV region into two or more clusters.

Before starting the FCM algorithm, the number of clusters, c, is set to the number of tissue types believed, by the expert, to make up the image being segmented. In general, c is image dependent. This number depends also on the type of images. A slice of given organ acquired by two different imaging techniques, such as MR and Emission Tomography (ET), does not exhibit exactly the same number of clusters. In MR imaging, clusters represent anatomical structures, while in ET, they represent regions of radioactive tracer uptake (functional regions). Nevertheless, the knowledge of the heart anatomy and the of organs and structures surrounding it allows us to estimate an adequate number of clusters. Even if the SA view is largely used, cardiac images to not exhibit the same anatomical structures for another view like the long axis view. Thus, the c number may be different from 6. Note that we have to segment the filtered image and to use the non-filtered one to calculate the LV area avoiding the partial volume effects. The discrepancy between the expert's EFs and those found automatically by the FCM seems due to flow variations. The difference may occur at papillary muscles whose presence in images is unpredictable [2]. It is important to keep in mind that delineating the left ventricular contours depends considerably on operator experience. The results reported here, though evaluated on the basis of only one expert opinion, indicate good performance. A large number of patients must be studied to confirm our findings. The inter- and intra-observer variations must be considered. Finally, the measurements found from cardiac MR imaging must be validated with respect to conventional contrast angiography to measure the algorithm performance.

Conclusion

Segmentation of cardiac MR images is a difficult problem because intensities in such images depend on the blood velocity as well as on the tissue types. A new method, based on the FCM model, for segmentation of such images is introduced. The aim is to delineate correctly the LV endocardial edges. This operation is important to evaluate parameters of the cardiac function. The edges detected by the proposed method have good correlation with the cardiac anatomy. However, it is well known that the main drawback with the FCM algorithm is that the exact number of clusters must be fixed before starting the clustering process. At the present time, there is no simple way to determine the adequate number of clusters. Furthermore, this method cannot extract the epicardial surfaces because portions of the heart walls and the surrounding tissues have similar intensities.

Acknowledgments

The author wishes to thank Dr. J. Champier for manuscript reading and Dr. J.C. Bordet for data acquisition.

References

1. MacMillan RM. Magnetic resonance imaging vs ultrafast computed tomography for cardiac diagnosis. Int J Cardiac Imag 1992; 8: 217–27.
2. Zimmer Y, Akselrod S. An automatic contour extraction algorithm for short-axis cardiac magnetic images. Med Phys 1996; 23: 1371–9.
3. Goshtasby A, Turner DA. Segmentation of cardiac cine MR images for extraction of right and left ventricular chambers. IEEE Trans Med Imag 1995; 14: 56–64.
4. Cohen LD. On active contour models and balloons. CVGIP: Image Understanding 1991; 53: 211–8.
5. Cohen LD, Cohen I. Finite element methods for active contour models and balloons. IEEE Trans Pattern Anal Mach Intell 1993; 15: 1131–47.
6. Staib LH, Duncan JS. Boundary finding with parametrically deformable models. IEEE Trans Pattern Anal Mach Intell 1992; 14: 1061–75.
7. Faber TL, Stokely EM, Peshock RM, Corbett JR. A model based four-dimensional left ventricular surface detector. IEEE Trans Med Imag 1991; 10: 321–9.
8. Suh DY, Eisner RL, Mersereau RM, Pettigrew RI. Knowledge based system for boundary detection of four dimensional cardiac magnetic resonance image sequences. IEEE Trans Med Imag 1993; 12: 65–72.
9. Fleagle SR, Thedens DR, Ehrhardt JC, Scholz TD, Skorton DJ. Automated identification of left ventricular borders from spin

echo magnetic resonance images. Experimental and clinical feasibility studies. Inv Radiol 1991; 26: 295–303.
10. Guttman MA, Prince JL, McVeigh ER. Tag and contour detection in tagged MR images of the left ventricle. IEEE Trans Med Imag 1994; 13: 74–87.
11. Hummel RA, Zucker SW. On the fundations of relaxation labeling process. IEEE Trans Patt Anal Mach Intell 1983; 5: 267–87.
12. Besag J. On the statistical analysis of dirty pictures. J Roy Stat Soc 1986; 48: 259–302.
13. Kasyhap RL, Chellappa R. Estimation and choice of neighbors in spatial interaction models of images. IEEE Trans Inform Theory 1983; 29: 60–72.
14. Prewitt JMS. Object enhancement and relaxation. In: Lipkin BS, Rosenfeld A, (eds). Picture processing and psychopictories. New York: Academic Press, 1970.
15. Rosenfeld A. The fuzzy geometry of image subsets. Patt Recogn Lett 1984; 2: 311–7.
16. Bezdek JC. Pattern recognition with fuzzy objective function algorithms. New York: Plenum, 1981.
17. Boudraa AEO, Mallet JJ, Besson JE, Bouyoucef SE, Champier J. Left ventricle automated detection method in gated isotopic ventriculography using fuzzy clustering. IEEE Trans Med Imag 1993; 12: 451–65.
18. Boudraa AEO. Images fuzzy segmentation: application to isotopic ventriculography, magnetic resonance imaging and positron emission tomography. PhD Thesis, University of Lyon, 1994.
19. Boudraa AEO, Champier J, Cinotti L, Bordet JC, Lavenne F, Mallet JJ. Delineation and quantitation of brain lesions by fuzzy clustering in positron emission tomography. Comput Med Imag Graph 1996; 20: 31–41.
20. Pedrycz W. Fuzzy sets in pattern recognition methodology and methods. Patt Recogn 1990; 23: 121–46.
21. Bezdek JC, Hathaway R. Recent convergence results for fuzzy *c*-means clustering algorithms. J Classification 1988; 5: 237–47.
22. Florentine MS, Grosskreutz CL, Chang W, Hartnett JA, Dunn VD, Ehrhart JC, Fleagle SR, Collins SM, Marcus ML, Skorton DJ. Measurement of left ventricular mass *in vivo* using gated nuclear magnetic resonance imaging. J Am Coll Cardiol 1986; 8: 107–12.
23. Keller AM, Peshock RM, Malloy CR, Buja LM, Nunnally R, Parkey RW, Willerson JT. *In vivo* measurement of myocardial mass using nuclear magnetic resonance imaging. J Am Coll Cardiol 1986; 8: 113–7.
24. Goshtasby A, Turner DA. Segmentation of cardiac MR images for extraction of right and left ventricular chambers. IEEE Trans Med Imag 1995; 14: 56–64.

Address for correspondence: Abd-El-Ouahab Boudraa, Laboratoire de Biophysique, Faculté de Médecine René Laënnec, rue Guillaume Paradin 69372 Lyon, Cedex 08, France